

Received February 27, 2020, accepted March 7, 2020, date of publication March 16, 2020, date of current version March 26, 2020.

Digital Object Identifier 10.1109/ACCESS.2020.2980869

# Design of Imperceptible Metamer Markers and Application Systems

KANGHOON LEE<sup>1</sup>, KYUDONG SIM<sup>1</sup>, TAEYOUNG UHM<sup>2</sup>, SANG HWA LEE<sup>3</sup>,  
AND JONG-IL PARK<sup>1</sup>, (Member, IEEE)

<sup>1</sup>Department of Computer Science, Hanyang University, Seoul 04763, South Korea

<sup>2</sup>Smart Mobility Research Center, Korea Institute of Robotics & Technology Convergence, Pohang 37666, South Korea

<sup>3</sup>Institute of New Media and Communications, Seoul National University, Seoul 08826, South Korea

Corresponding author: Jong-Il Park (jipark@hanyang.ac.kr)

This work was supported by the National Research Foundation of Korea (NRF) Grant funded by the Korean Government (MSIT) under Grant NRF-2019R1A4A1029800.

**ABSTRACT** This paper presents a application system using imperceptible metamer markers. The proposed system is based on metamer markers that are invisible to the human eye but visible to infrared (IR) cameras. The metamer means the indistinguishable colors with different spectrums. RGB cameras cannot capture the different spectrums of metamer markers, but IR cameras can detect the metamer markers printed under the color image. This paper describes how to create metamer markers using a ordinary color printer. First, uniformly select color samples from the RGB color space, analyze the visibility of RGB colors and metamer color printed by the printer, and then design a color mapping model between color printers to produce the effective metamer color. After confirming successful detection of a metamer marker under various infrared lightings and filters, the exact color differences were analyzed and the validity of the proposed method was clarified. To verify its applicability, a prototype of fairytale book was published and demonstrated as an AR-book. The metamer markers are expected to be very useful for AR applications, projector-camera systems, human-computer interaction systems, and so on.

**INDEX TERMS** Metamer marker, imperceptible marker, augmented reality, infrared imaging, color correction, projection system.

## I. INTRODUCTION

Recently, various augmented and mixed reality (AR/MR) systems became available for consumers as the performance of sensor devices and processing hardware improved. Interest in AR and MR systems is also prevalent among ordinary consumers, and the need for various consumer applications has also increased. To develop AR/MR systems, many technologies and subsystems are required, such as projectors, high-resolution displays, user interfaces, pattern recognition techniques, sensor fusion and calibration, realistic 3D graphics and rendering, and interactive content [1]–[5]. This paper focuses on marker-based user interaction systems for various AR/MR applications. In particular, this paper deals with natural and invisible markers for displaying or projecting visual content.

Projectors have been used as consumer electronics, displaying visual contents. Studies on a combined system

The associate editor coordinating the review of this manuscript and approving it for publication was Fabrizio Marozzo<sup>1</sup>.

of mobile projectors and cameras have been extensively explored recently. Researches for utilizing it in HCI(Human-Computer Interaction) and VR(Virtual Reality) [6] and developing spatial immersion displays [7] have affected the progress of projector-camera system. Also technology of projection-AR and associated research were performed to recognize markers or objects [2], [3], [8]. Since then, the projector-camera system has been widely developed in many aspects, such as geometric correction [9] and color correction [10] interaction through handheld-projector [11], projection AR applied to the theme park [12], enhancing game experiences [13], infrared ink markers and camera [14]–[16].

Markers have been used to implement practical AR systems for decades. The natural markers are unobtrusively embedded in the visual content so that the users rarely recognize the existence of markers. The natural markers can be divided into two types: one is a marker-less type and the other is an invisible marker (that is to say, there are specific shapes of markers in the image, but they are not visible). In the case of the marker-less type, the markers are not specifically

designed, and image features such as corners and edges are exploited as component of the markers. The features of markers are described from an image analysis around the marker position, such as SIFT [17], SURF [18], BRIEF [19], and ORB [20]. This marker-less type is mainly dependent on the image contents, and the feature points are changed as the image contents vary. Thus, it is important to detect the feature point position repeatedly under image variation. Since new feature points should be defined as a relation to image contents, a configuration of contents is restricted and therefore complexity and robustness issues arise in the design of AR application and utilization of interaction.

Some fixed shapes of markers are more useful when we design interactions regardless of images contents. The most popular markers are the AR markers designed like 2D QR codes. There have been various studies such as these QR codes propose a color barcode framework for mobile applications [21]. However, these kinds of AR markers are remarkably visible in the image contents, which obstructs users' immersion. In order to solve these drawbacks, research on invisible markers has been advanced. Invisible markers are used in AR by two different approaches: hiding it in images or physical coverage. The way to hide in images is performed by inpainting the parts of markers on the user's screen [22], [23]. This is an indirect method. The physically hiding method uses data hiding in clustered-dot halftone [24], watermark from halftone dots method [25], and the markers consisting of retro-reflectors [26], all of which are light change sensitive. QR codes can be printed out using UV ink then text or picture is covered on top of the ink [27]. There is also a method of using fluorescence characteristics that are only visible under UV lighting [28], [29]. Since it requires specific ink and printer and harmful electromagnetic field, it is hard to apply to ordinary consumer products. Also, UV lighting is not used very much. On the other hand IR camera and lights are widely used in many fields. Due to the invisible feature of infrared, it has been applied to a variety of applications, for instance, marker tracking for AR [30], pose estimation [31], fear therapy for small animals [32], and utilization of mobile projectors [14]. Recently, marker research using radiometric compensation technology has been conducted [33].

To make invisible markers, some systems used IR pens and ink that absorb the IR spectrum band [14], [30], [34]. When the IR cameras capture the images with IR markers, the regions of IR markers are very dark since IR spectrums are absorbed. These kinds of IR markers are natural, but the users have to draw the markers with IR ink or pen under exposure of some poisonous chemical materials. In addition, the optimal density of IR ink is dependent on the toner types of color printers that are used to print color images over the IR ink markers. Thus, it is difficult to make the IR markers consistently. Fig. 1 shows an example of IR markers using IR ink and a color printer. The IR markers were drawn with IR ink, and the color image was printed over the IR markers. The IR markers are shown and diffused a bit on the color image. Actually, handling the print strength of IR markers is

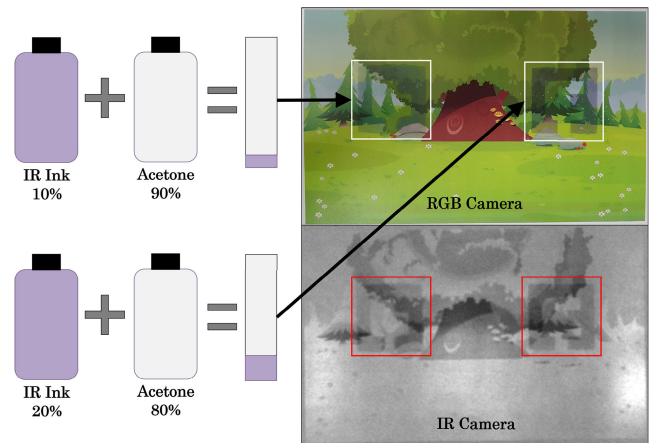


**FIGURE 1.** Example of IR ink markers on the color image. (left) IR ink dilution rate. (top right) IR marker is first drawn on the paper, and then color image is printed over the markers. The IR ink is shown on the color image. (bottom right) IR camera image of color image. According to the used color toners, the colors near IR bands are also shown, which deteriorates IR marker tracking.

not trivial work since the density of IR ink should be adjusted with respect to the printed colors and printer toners. IR ink is very dark and should be diluted for use. Fig. 1 shows a marker and a color print of IR ink diluted at 10 percent and 20 percent. Even when the IR ink is diluted to 10 percent, the markers are visible.

This paper proposes how to create invisible metamer markers with ordinary color printers. The metamer means the indistinguishable colors with different spectrums [34], [35]. The main concept of the proposed metamer markers is based on the observation that the IR spectrum strengths are different when a same color is printed with different printers [36]. This paper is an extension of the previous work [36] to improve imperceptibility of color difference in visible range while maintaining differences in infrared range. There is a certain amount of color spectrum difference between two printed materials of the same image from different printers, which allow the human eyes or the color cameras can notice the color difference. Thus, if the color models of both printers are analyzed and appropriately deformed, they can be printed in visually similar colors. However, the difference of the IR spectrum is maintained to distinguish the marker from the background color image. Color correction is defined as the modification of color model applied in digital images, display and printing. A variety of methods and applications have been progressed in multiple areas, for instance, CIELAB image printing by Trilinear Interpolation [37], changes of spatial colors by Trilinear Interpolation [38], application of one-color feature into other image cases [39], printer color correction using LUT (Look-Up Table) [40], Color conversion to create color images visible only under UV light [2R2-41], and Halftone color analysis printed on paper containing fluorescent brighteners [42].

The main contribution of this paper is to handle the color mapping between two printers in order to make invisible metamer markers with the usual color printers

and to implement plausible projection systems based on the principle. Users can easily create metamer markers on common printers using the proposed color mapping model. Well-known AR toolkit markers, QR codes, and Bar-codes can be easily used as the shape of markers. In this paper, we propose a new color correction method based on a piecewise approximation of overall color mapping model. While adjusting the visible colors look similar, we tried to keep the difference of IR spectrums maintained to distinguish the markers through IR cameras.

A fairytale book (asia zodiac signs story) that can be used in various camera-projector based e-learning systems was created to show the application effects of the metamer marker proposed in this paper. And we built a camera-projector system and demonstrated that e-learning content videos were projected according to the recognized markers.

The rest of paper is organized as follows. Section II describes the proposed basic approach to make invisible IR markers using different printers. Section III explains the color mapping models which make the printed markers more invisible on the color images. Section IV shows the implemented application with projector system. This paper concludes with Section V.

## II. OVERLAID PRINT OF IR METAMER MARKER

### A. DIFFERENCE OF IR VISIBILITY IN THE PRINTERS

Though the same colors are printed on the paper, the spectrum of IR band can be different with respect to the toners and ink. The visual light spectrum bands are almost same with two printed colors, but the IR spectrum bands show a bit difference. This metamer phenomena become more apparent especially when inkjet and laserjet printers are used to print the same color. This is mainly caused by the difference in the amount of carbon contained in the ink and toner manufacturing processes. The point to be noted in this paper is that even if the same color is printed, the marker part is printed by another printer, so it is invisible to the naked eye, but the marker can be detected and discriminated by the IR camera.

This paper has performed compare experiments with four printers of different manufacturers in order to compare with the visibility of markers in the IR spectrum bands. Inkjet printers are named A(EPSON L805) and B(HP OfficJet 8640) printers, and laser printers are C(CANON MF8000c) and D(ZEROX ColorQube 8570). The left side of Fig 2 shows the IR camera image of the markers printed by four different printers. As we can see in Fig. 2(left), the visibility of markers in the IR spectrum bands is different with respect to the property of toner and ink. The printer types B and C are suitable for marker printing since they are well shown in the IR cameras. On the left side of Fig 2, one color image was printed by four different printers and then captured by an IR camera. The IR visibility of printer types A and D is relatively small. Thus, the printer types A and D are suitable for printing color images. And the dark colors tend to be highly visible from IR cameras.

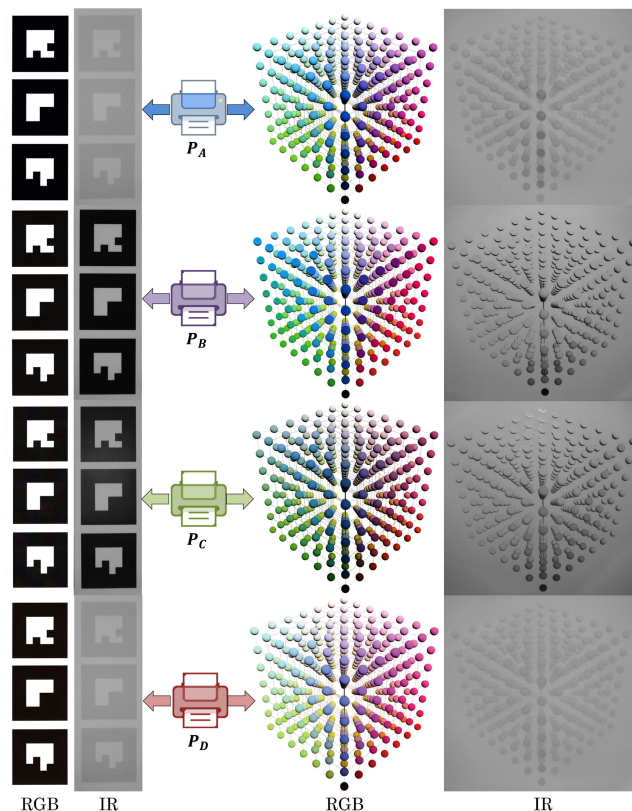


FIGURE 2. IR images of black marker and color image printed with four different printers. The visibility of the IR spectrum bands differs with respect to the printer toner and ink types.

### B. PRINTING IR METAMER MARKERS

The proposed concept of metamer markers in this paper is to use printers that have different IR visibility. When the markers are printed with printers of high IR visibility and the color image is printed over the markers with printers of low IR visibility, IR cameras captures the marker well. This makes it possible to produce a marker that is invisible to the naked eye using a ordinary color printer.

The method of making the existing invisible markers is to print the markers and cover them with white spray on the printed markers so that the markers are not visually visible. However, the spray areas have a lower quality of the color image printing. Also IR making one marker takes a lot of time and the process is complicated. For these reasons, the IR markers with consistent quality are not guaranteed.

Figure 3 shows the proposed concept of making metamer markers. In Fig. 3, the subfigure (a) shows the printed markers with printer type C in Fig. 2 and its IR camera image. The Fig.3 (b) shows the color image printed with printer type A and its IR camera image. Finally, Fig. 3 (c) is the overlaid printing and its IR camera image. As we can see in Fig. 3, the marker is only shown regardless of color image contents. At this time, since the black marker is very often seen by the naked eye, the gray scale value needs to be adjusted. As a result of repeated experiments, stable detection was

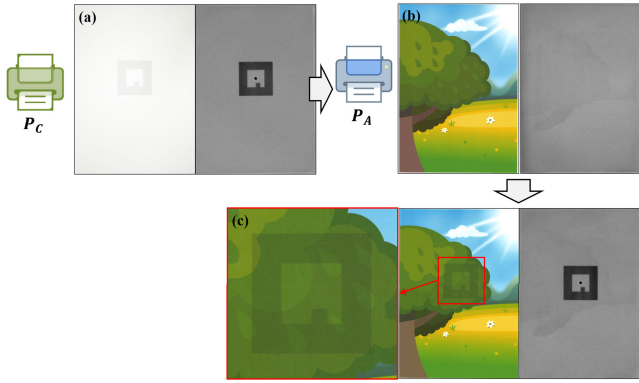


**FIGURE 3.** Proposed method to make metamer markers. (a) Marker printing with printer type C in Fig. 2 and its IR captured image, (b) color image printing with printer type A in Fig. 2 and its IR captured image, and (c) overlaid printing of (a) and (b), and its IR captured image.

possible even with a gray scale value of 229. One more need is a process of correcting and printing the original colors so that possible markers are not visible in the overprinted color image. The use of a color mapping model for that purpose makes it possible to make the markers less visible in the visible spectral bands.

### III. COLOR MAPPING MODELS

#### A. COLOR CORRECTION ALGORITHM

To create the suggested imperceptible markers, use two printers that can be distinguished in the IR band. Marker areas can be detected in IR images by using two printers to print marker areas and other areas. However, a problem occurs when printing one image using two printer with different printing colors. Images printed on two different printers that use ink or toner look different. Because an image was printed on two printers, the color difference in marker boundaries found in the image is indicative of the presence of the marker. To solve this problem, a color correction algorithm is required to print images of the same color with two printers. In this paper an algorithm of the color correction was produced by analyzing previous literature on color model correction and applying Trilinear-Interpolation and LUT method for three-dimensional color space [37]-[40].

As shown in Fig. 4, the color conversion and correction are designed using the RGB values of the original color and the RGB values of an image obtained by printing the original color with a printer and photographing again with a color camera. The printing color was photographed using a VC-12MC-C65EO (Body) and a Nikon AF-S Micro NIKKOR 60mm f/2.8G ED (Lens). In this paper, in order to select the RGB color space uniformly, select color samples of 343 ( $7 \times 7 \times 7$ ) in total, 7 at even intervals for each color channel, generate a color chart image, and printed on printer. Distortion of brightness and camera color may occur when shooting color chart, but the same applies to two images printed by different printers, minimizing the effect on color conversion and calibration. The color correction algorithm

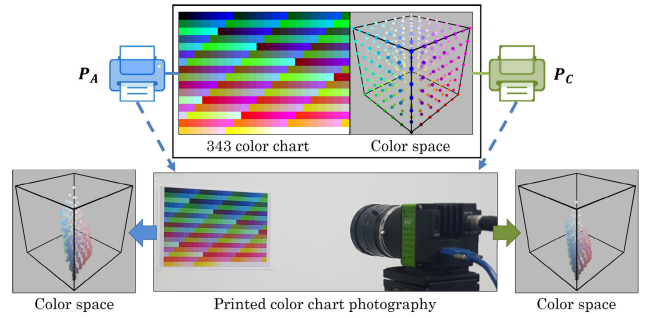


**FIGURE 4.** Sample color chart and camera image. (left) Generated color patches and (right) captured color patches.

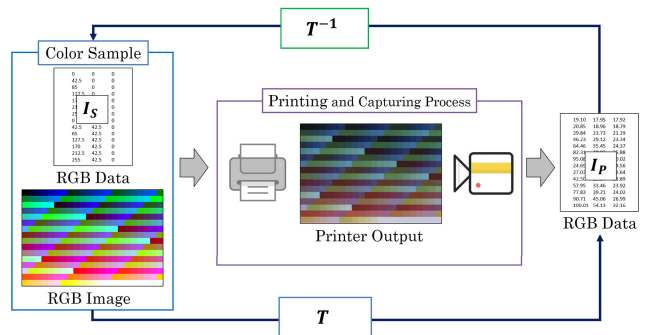


**FIGURE 5.** The relationship of the printer color representation of a computer image.  $T$  conversion relation and  $T^{-1}$  conversion relation.

uses two types of color information to determine before and after color correction. Fig. 5 shows a process of correcting using a difference in color information. The color representation and area of the printer can be determined from two kinds of color information, and the RGB image printed on two printers has different color information. Additionally, for color samples for the color conversion, a total of 343 color samples are used; these are collected by extracting 7 samples in equals interval from a 3-channel RGB color. Therefore, the relationship between the two pieces of color information includes the color representation of the printer. There are two algorithms for the color conversion. One of them is  $T$  conversion that finds the printed color chart RGB data ( $I_P$ ) from the original color chart RGB data ( $I_S$ ), and the other one is  $T^{-1}$  conversion that finds the original color chart RGB data ( $I_S$ ) from the printed color chart RGB data ( $I_P$ ). This process is performed in printers  $P_A$  and  $P_C$ , respectively.

Because the number of RGB data  $I_S$  and  $I_P$  is the same, 343 colors of the sample are 1: 1 mapped, and the values between them are forward mapped using linear interpolation in three dimensions using the mapped color information. As shown in Fig. 5, color data can be  $T$  transformed using linear interpolation and forward mapping. The  $T^{-1}$  conversion is a transformation that converts the output image RGB data to the original image RGB data. The color not in the color patch is inferred in the same manner as in Fig. 6 when each  $S_{(1-8,d)}$  and  $S_{(1-8,p)}$  represents and prints the RGB value of the color patch of digital data.

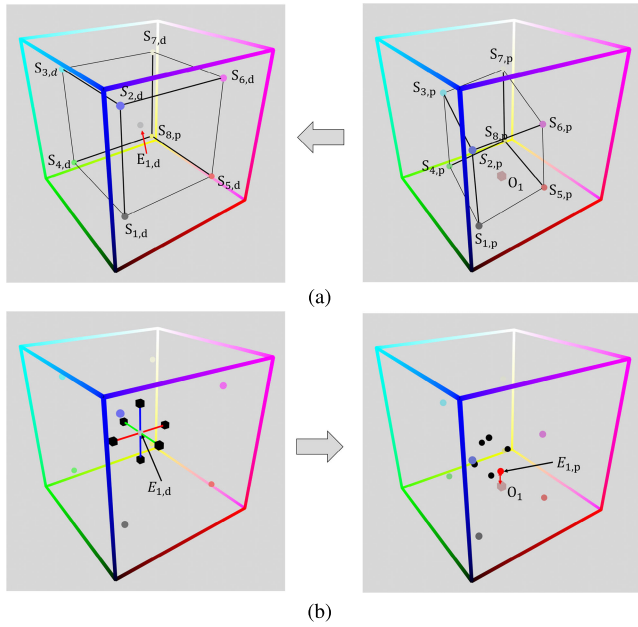


**FIGURE 6.** Expression of color correction (mapping) method in color spaces between pure color data and printed color data.

To find the point that the printed digital color is  $O_1$ , the sample color value  $S_{(1-8,p)}$  near  $O_1$  will be selected in a color chart, thereby finding out RGB data  $S_{(1-8,d)}$  of an original color chart. Fig. 6 (a) shows the sample colors  $S_{(1-8,d)}$  and  $S_{(1-8,p)}$  placed in the virtual space. The  $T$  and  $T^{-1}$  conversions between the original RGB data and the printed RGB data are not linear. Accordingly, the RGB value which is  $T$  transform of digital RGB  $O_1$  deduced from the sample color  $T^{-1}$  is different from the RGB value of  $O_1$ , and there is also a color difference.

In order to deduce RGB value of  $O_1$ ,  $E_{(1,d)}$  located at the center of  $S_{(1-8,d)}$  are selected and  $T$  transformed so that  $E_{(1,p)}$  can be obtained. However, the RGB value of  $E_{(1,p)}$  is different from that of  $O_1$ , so the distance between them is far apart from each other in the color space. For the reduced distance in the space, points in both directions of each R, G, B axis (6 directions) are moved certain distances in the 3-dimensional space around  $E_{(1,d)}$ . Each point  $E_{(1,d)}$  moved to six directions is transformed to select the closest one with the color space  $O_1$ . (see Fig. 6 (b)) The selected points are  $E_{(2,d)}$  and  $E_{(2,p)}$ , respectively. Repeat these processes  $n$  times. If there is no reduction, terminate the process. As a result,  $O_1$  is expected to be printed by printing  $E_{(n,p)}$ . The whole process of finding  $E_{(n,d)}$  and  $E_{(n,p)}$  to obtain  $O_1$  is  $C$  correction. This process is performed for each pixel of the image.

The two types of color conversion suggested above include the color representation space of the printer and they are used to print an image of the same color. Because the color space expressed in the two printers is different, the image can be seen differently when printing the image, but if the color space prints different images, it can be seen in the same color. Using those two types of color conversion makes it possible to print the same color with two printers. The information of

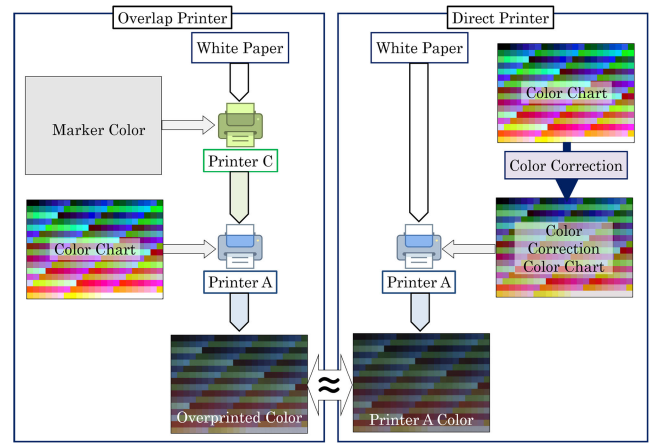


**FIGURE 7.** Color conversion the same color printing process by  $C$  correction. (left) after printing the marker color, color patch overprint (The marker is printed as a whole background), (right) printed color patches without marker color.

the colors printed by two printers is obtained by  $T_1$  conversion and  $T_2$  conversion, and the images printed by the two printers becomes identical due to  $C$  correction. Each image printed with two printers is identical to equation (1).

$$T_1(C(I_s)) = T_2(I_s) \quad (1)$$

When  $T^{-1}$  conversion is used, it can be explained by equation (2).

$$C(I_s) = T_1^{-1}(T_2(I_s)) \\ C = T_1^{-1}T_2 \quad (2)$$

$C$  correction can be obtained from conversion equations of two printers. Thus, using the  $C$  correction, the original data can be output to a separate image to each printer to obtain a similar looking output colors. However, there are a few constraints for the usage of  $C$  correction. As two printers have different color gamuts, a color that one of the printers can express cannot be expressed by the other one. Therefore, the color space expressible by both needs to be used, and as the color gamuts of the two printers used during the research have a subordinate relationship,  $C$  correction from the printer with a wide color gamut to the one with a narrow color gamut is used. Therefore, it is desirable to cover with one printer.

As mentioned above, metamer markers use two types of printers. However, if printers with different printing methods are used, the difference increases, as the print surface glossiness of the laser printer is higher than that of the inkjet printer. Therefore, it is desirable to cover with one printer. Markers and background images were printed based on the method of Fig. 3 to reduce differences due to surface gloss. At this time, the overprinted color is named a printing color of the overlap printer, and if the same as the original color chart RGB data, the overlap printer  $T$  conversion relationship is established. Therefore,  $C$  correction can be performed. (see Fig. 7). When correcting the image of the overlap printer, the image is slightly brightened. However, when the color of the background image is bright, the gray marker cannot

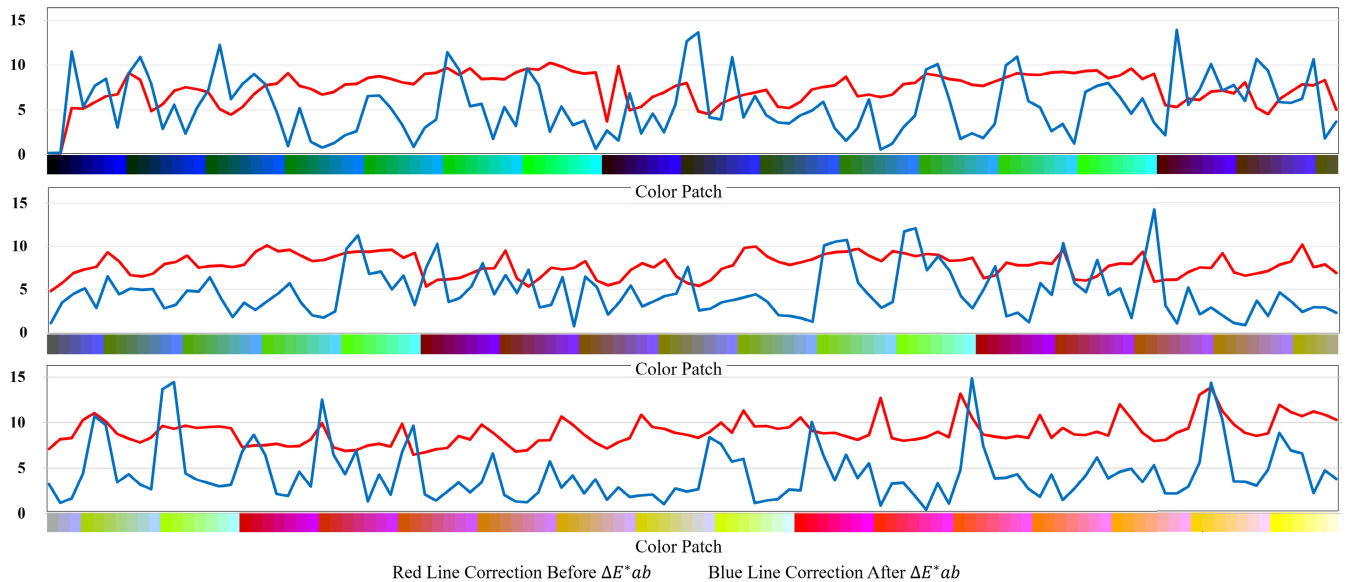


**FIGURE 8.** Comparison of color difference using a spectrophotometer. We divided the 343 color charts into 3 parts to display the  $\Delta E^*ab$  values for each color. The red line is the color difference when color correction is not performed. The blue line is the color difference at the time of color correction.

be hidden. Therefore, the image of the part, not the marker, is corrected, and the color is slightly darkened. The degree of brightening or darkening varies depending on the color, so  $C$  correction needs to be performed.

## B. DATA ACQUISITION

The algorithm suggested above makes revisions that result in images of the same color with two printers, but it is difficult to gain the desired result with an algorithm. The accuracy of post-printing data and pre-printing data used in the algorithm needs to be ideal but post-printing color data is prone to errors. To measure a printed color precisely, whether there is no errors with the output or with image gain can be separately considered. Maintained printer settings and printing software settings to always output a constant color.

A lot more needs to be taken into consideration to keep the image gain steady. Noise and the consistency of lighting are typical problems. The noise from image gain can be overcome by averaging sufficient numbers of color information. In this paper, noise was overcome by taking a total of two steps, such as taking 100 images, obtaining an average image, and obtaining the average value of multiple pixels for each 343 color chart. In order to overcome the influence of the lighting environment, the whiteboard was placed in an environment where a color chart was shot, and the brightness of the whiteboard was changed. The color patches were similarly corrected based on the information that the brightness of the whiteboard changes according to the lighting environment, so that even if the lighting environment was not completely uniform, it was corrected as if the lighting environment were the same. In fact, the environment for photographing the two types of color charts was set as identical as possible. The photographing was performed at the same place indoors

at the same night time so that the lighting environment for photographing was the same.

The information of 343 colors acquired through the above procedures is sufficiently accurate to apply the proposed algorithm and also shows that the IR marker detection system can operate ideally. To confirm the improvement due to the color correction, the color chart was measured using a spectrophotometer (Konica Minolta CM-2600d). Fig. 8 is a comparison of color difference using a spectrophotometer. A spectrophotometer was used to confirm the improvement of color correction. The blue line indicates the color difference value between the color of the marker printed on the printer C and the color chart overprinted on the printer A and the corrected color chart printed on the printer A. The red line is the color difference value from the uncorrected color chart. The color difference,  $\Delta E^*ab$ , from the non-correction color chart was 8.09. The color difference,  $\Delta E^*ab$ , from the color chart after correction was 4.88. The color correction algorithm proposed in this paper shows that the color difference has greatly decreased. It is predicted that some  $\Delta E$  values are large due to errors in the data acquisition phase or the measurement phase.

The metamer marker proposed in this paper was fabricated as shown in Fig. 9. First, the marker area is printed by the printer C in which the marker in the IR spectrum band is clearly visible. Next, the color image is printed on a printer A whose color cannot be seen by the IR camera. The marker area uses the original color image as it is, and the non-marker area uses a corrected color image.

## IV. METAMER MARKER APPLICATION

Metamer markers can be applied and used in various fields. We created a stand-type projection system to utilize the

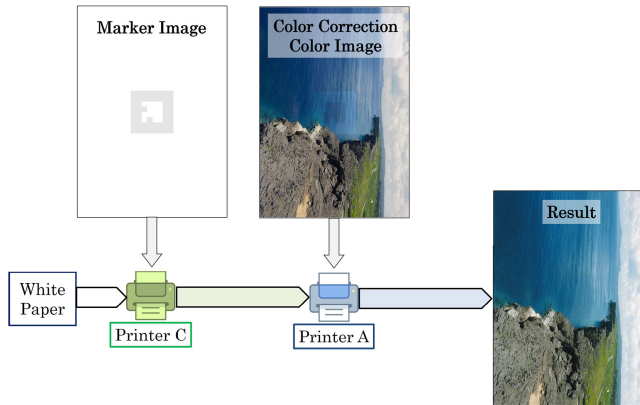


**FIGURE 9.** Concept of color correction for invisible metamer marker printing. The color spaces of two different printers are converted.

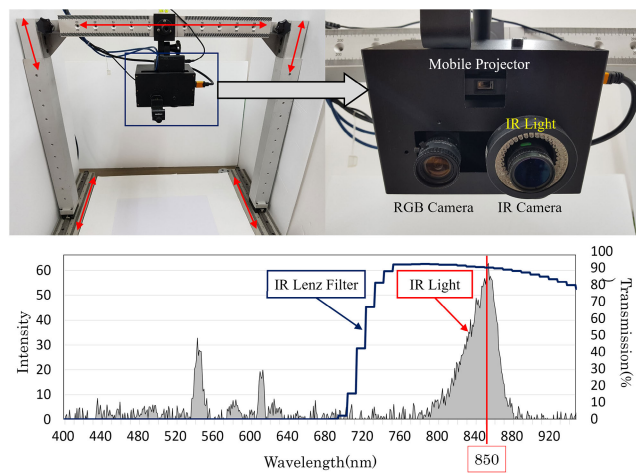
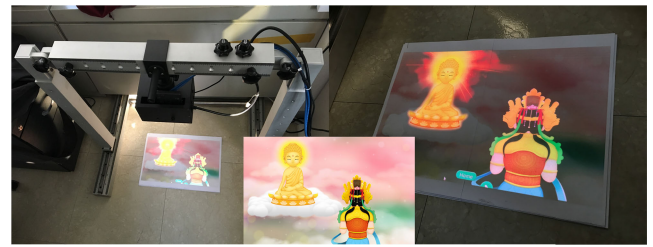


**FIGURE 10.** Application system of proposed metamer markers. (Top) The system consists of an IR camera, an IR light, an RGB camera, and a projector. (Bottom) IR light.

metamer markers. The projection system consists of a mobile projector (Sony MP-CL1A) to project video content onto a color image plane, an RGB camera (Flea3 FL3-U3-13E4C 1280 × 1024) to calibrate cameras and the projector, and an IR camera (Flea3 FL3-U3-13E4M 1280 × 1024) with IR light to track the metamer marker (see Fig. 10 (Top-right)). Since it is produced in a form of table stand, the stand can shift to all x-, y-, and z-axis while the projector-camera module can be rotated through 180 degrees (see Fig. 10 (Top-left)). IR cameras and IR lights used to trace markers were tested with various infrared filters and lighting. The infrared lens filter used a band pass between 780 nm and 900 nm. As shown at the bottom of Fig. 10 (Bottom), IR illumination was used at a maximum of 855 nm in the infrared area. IR light intensity measurements were made using a spectroradiometer (Luzchem SPR-03).

In order to demonstrate the projection system, an imperceptible metamer marker application test was conducted. The scenario of the application system is to project video content onto the color image plane whenever the metamer markers are recognized. The AR Interactive-system can be used to



(a)



(b)

**FIGURE 11.** The geometric relationship of the printed image and the projector is calibrated, and the video content is projected at the exact location of the printed image. (a) Projector camera system test (b) Capture Fairy tale AR-book video content projection scene.

print a fairy tale book as a purpose of education [43], [44]. Several color background pictures images and video contents are designed with respect to the marker shapes. Fig. 11(a) shows captured scenes of projected video content on the color image. The projection of video content does not affect the metamer marker tracking since the lighting spectrum of the projector is mainly the visible light band. In the implemented application shown in Fig. 11(b), the metamer markers play a role in displaying interactive content. Since the metamer markers are not visible in the color images, users can better immerse themselves in the content. The proposed system can be applied to the smart-projection system, enabling you to do projection into any position that you want. Fig. 12(a) are one of the examples that overlaid on a poster of walls. This concept can be expanded by considering transferability. Fig. 12(b) is a conceptual diagram of a moveable projection system.

Metamer markers can be applied to various backgrounds because they can be applied to photographic images, not graphic images. Fig. 13 shows the result of applying a photographic image, not a graphic image. If color correction is not done, the RGB image shows traces of markers Fig. 13(RGB1). When color correction is performed, the markers in the photograph are almost invisible to the naked eye, but the marker can be clearly distinguished in the IR image (see Fig. 13(IR)). Nevertheless, it is not easy to completely hide the metamer markers in all background images.

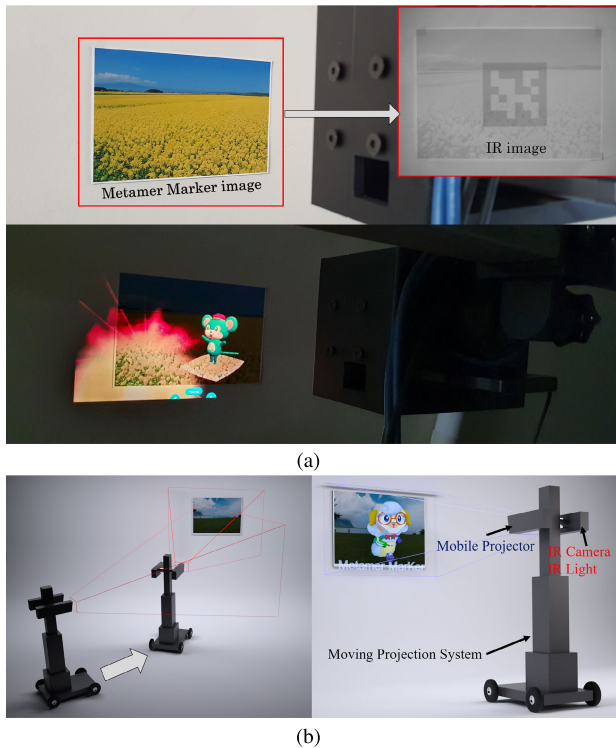


FIGURE 12. (a) Projection on a Wall with Markers (b) Movable type projection system.



FIGURE 13. Metamer marker applied to the photo. (RGB-1) Overlaid printing of photos and marker, (RGB-2) Overlaid printing of color-corrected photos and marker, (IR) Infrared camera image (RGB Captured by mobile phone S10+).

In Fig. 13(RGB2-left), the trace of the markers appear weak. These results are because it is difficult to completely hide the light gray of the marker when the background image is a monotonous bright color. On the other hand, it is not easy to find markers from complex background images or dark backgrounds (see Fig. 13(RGB2-right)). There is also an influence by the spectral characteristics of the photographed device. Particularly when using a scanner, small marks on the marker are noticeable due to the influence of the illumination of the scanner. In an environments where it is not easy to

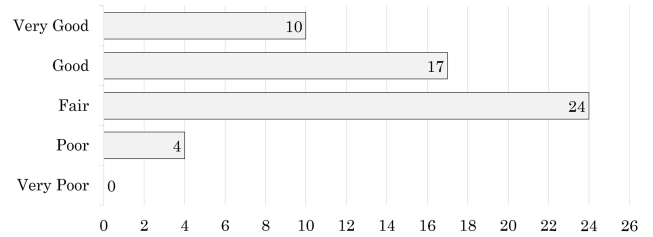


FIGURE 14. Metamer marker user quality assessment results.

distinguish metamer markers with the naked eye, it was not easy to distinguish them with a digital camera.

Finally, we evaluated the visibility of metamer markers in 55 men(38 people) and women(17 people) between the ages of 20 and 27 years. The evaluators compared and evaluated what was printed with metamer markers and what was not. Visually assessed metamer marker quality was 49 percent for Very Good and Good, 44 percent for Fair, and 7 percent for Poor and Very Poor(see Fig. 14).

## V. CONCLUSION

The proposed markers are detected in the printed image by IR cameras, but not visible to general color cameras or human eyes. This paper has designed the printer color mapping method to generate proper metamer colors since the invisible colors of metamer markers depend on the printed background colors. A test that demonstrates an initial concept, including color difference analysis resulting from metamer marker detections and color corrections in the infrared images, showed that the metamer marker was effective. Applications of the projection system based on the metamer marker was proved that by publishing a Fairytale book and demonstrating it with a projection-AR book. It suggested a concept about the mobile projection-system which can be used in various fields. In the future study, it would be an improved intelligent projection system that includes geometric correction caused by brightness correction and nonplanar projection which consider user's environment.

## REFERENCES

- [1] R. T. Azuma, "A survey of augmented reality technologies, applications and limitations," *Presence, Teleoperators Virtual Environ.*, vol. 6, no. 4, pp. 355–385, 1997.
- [2] R. Azuma, Y. Baillot, R. Behringer, S. Feiner, S. Julier, and B. MacIntyre, "Recent advances in augmented reality," *IEEE Comput. Graph. Appl.*, vol. 21, no. 6, pp. 34–47, Dec. 2001.
- [3] D. W. F. Van Krevelen and R. Poelman, "A survey of augmented reality technologies, applications and limitations," *Int. J. Virtual Reality*, vol. 9, no. 2, pp. 1–20, 2010.
- [4] F. Zhou, H. B.-L. Duh, and M. Billinghurst, "Trends in augmented reality tracking, interaction and display: A review of ten years of ISMAR," in *Proc. 7th IEEE/ACM Int. Symp. Mixed Augmented Reality*, Cambridge, U.K., Sep. 2008, pp. 193–202.
- [5] M. Billinghurst, A. Clark, and G. Lee, "A survey of augmented reality," *Found. Trends Hum.-Comput. Interact.*, vol. 8, nos. 2–3, pp. 73–272, 2015.
- [6] P. Wellner, "Interacting with paper on the DigitalDesk," *Commun. ACM*, vol. 36, no. 7, pp. 87–96, Jul. 1993.
- [7] R. Raskar, G. Welch, M. Cutts, A. Lake, L. Stesin, and H. Fuchs, "The office of the future: A unified approach to image-based modeling and spatially immersive displays," in *Proc. 25th Annu. Conf. Comput. Graph. Interact. Techn.*, 1998, pp. 179–188.



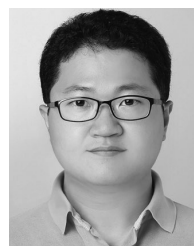
- [8] O. Bimber and R. Raskar, *Spatial Augmented Reality: Merging Real Virtual Worlds*. Boca Raton, FL, USA: CRC Press, 2005.
- [9] R. Raskar, J. van Baar, P. Beardsley, T. Willwacher, S. Rao, and C. Forlines, "iLamps: Geometrically aware and self-configuring projectors," *ACM Trans. Graph.*, vol. 22, no. 3, pp. 809–818, 2003.
- [10] O. Bimber, D. Iwai, G. Wetzstein, and A. Grundhöfer, "The visual computing of projector-camera systems," *Comput. Graph. Forum*, vol. 27, no. 8, pp. 2219–2245, 2008.
- [11] P. Beardsley, J. van Baar, R. Raskar, and C. Forlines, "Interaction using a handheld projector," *IEEE Comput. Graph. Appl.*, vol. 25, no. 1, pp. 39–43, Jan. 2005.
- [12] M. R. Mine, J. van Baar, A. Grundhofer, D. Rose, and B. Yang, "Projection-based augmented reality in disney theme parks," *Computer*, vol. 45, no. 7, pp. 32–40, Jul. 2012.
- [13] B. R. Jones, H. Benko, E. Ofek, and A. D. Wilson, "IllumiRoom: Peripheral projected illusions for interactive experiences," in *Proc. ACM SIGGRAPH Emerg. Technol. (SIGGRAPH)*, 2013, pp. 869–878.
- [14] K. D. D. Willis, T. Shiratori, and M. Mahler, "Hideout: Mobile projector interaction with tangible objects and surfaces," in *Proc. TEI*, 2013, pp. 331–338.
- [15] P. Punpongsanon, D. Iwai, and K. Sato, "Projection-based visualization of tangential deformation of nonrigid surface by deformation estimation using infrared texture," *Virtual Reality*, vol. 19, no. 1, pp. 45–56, Mar. 2015.
- [16] G. Narita, Y. Watanabe, and M. Ishikawa, "Dynamic projection mapping onto deforming non-rigid surface using deformable dot cluster marker," *IEEE Trans. Vis. Comput. Graphics*, vol. 23, no. 3, pp. 1235–1248, Mar. 2017.
- [17] D. G. Lowe, "Distinctive image features from scale-invariant keypoints," *Int. J. Comput. Vis.*, vol. 60, no. 2, pp. 91–110, Nov. 2004.
- [18] H. Bay, A. Ess, T. Tuytelaars, and L. Van Gool, "Speeded-up robust features (SURF)," *Comput. Vis. Image Understand.*, vol. 110, no. 3, pp. 346–359, Jun. 2008.
- [19] M. Calonder, V. Lepetit, C. Strecha, and P. Fua, "BRIEF: Binary robust independent elementary features," in *Proc. Eur. Conf. Comput. Vis.*, 2010, pp. 778–792.
- [20] E. Rublee, V. Rabaud, K. Konolige, and G. Bradski, "ORB: An efficient alternative to SIFT or SURF," in *Proc. Int. Conf. Comput. Vis.*, Nov. 2011, pp. 2564–2571.
- [21] H. Blasinski, O. Bulan, and G. Sharma, "Color barcodes for mobile applications: A per channel framework," *IEEE Trans. Image Process.*, vol. 22, no. 4, pp. 1498–1511, Apr. 2013.
- [22] O. Korkalo, M. Aittala, and S. Siltanen, "Light-weight marker hiding for augmented reality," in *Proc. IEEE Int. Symp. Mixed Augmented Reality*, Oct. 2010, pp. 247–248.
- [23] N. Kawai, M. Yamasaki, T. Sato, and N. Yokoya, "[Paper] diminished reality for AR marker hiding based on image inpainting with reflection of luminance changes," *ITE Trans. Media Technol. Appl.*, vol. 1, no. 4, pp. 343–353, 2013.
- [24] O. Bulan, G. Sharma, and V. Monga, "Orientation modulation for data hiding in clustered-dot halftone prints," *IEEE Trans. Image Process.*, vol. 19, no. 8, pp. 2070–2084, Aug. 2010.
- [25] C.-H. Son and H. Choo, "Watermark detection from clustered halftone dots via learned dictionary," *Signal Process.*, vol. 102, pp. 77–84, Sep. 2014.
- [26] Y. Nakazato, M. Kanbara, and N. Yokoya, "Localization of wearable users using invisible retro-reflective markers and an IR camera," *Proc. SPIE*, vol. 5664, pp. 563–570, Mar. 2005.
- [27] K. Kamijo, N. Kamijo, and Z. Gang, "Invisible barcode with optimized error correction," in *Proc. 15th IEEE Int. Conf. Image Process.*, Oct. 2008, pp. 2036–2039.
- [28] Y. Zhao and R. Bala, "Printer characterization for UV encryption applications," in *Proc. 16th Color Imag. Conf.*, Nov. 2008, pp. 79–83.
- [29] R. Eschbach, R. Bala, and S. Wang, "Creating variable data UV signals for security applications," *Proc. SPIE*, vol. 6807, p. 68070K, Jan. 2008.
- [30] H. Park and J.-I. Park, "Invisible marker based augmented reality system," *Proc. SPIE*, vol. 5960, pp. 501–508, Jun. 2006.
- [31] T. Pintaric and H. Kaufmann, "Affordable infrared-optical pose tracking for virtual and augmented reality," in *Proc. Trends Issues Tracking Virtual Environ. Workshop*, 2007, pp. 44–51.
- [32] M. C. Juan and D. Joele, "A comparative study of the sense of presence and anxiety in an invisible marker versus a marker augmented reality system for the treatment of phobia towards small animals," *Int. J. Hum.-Comput. Stud.*, vol. 69, no. 6, pp. 440–453, Jun. 2011.
- [33] H. Asayama, D. Iwai, and K. Sato, "Fabricating diminishable visual markers for geometric registration in projection mapping," *IEEE Trans. Vis. Comput. Graphics*, vol. 24, no. 2, pp. 1091–1102, Feb. 2018.
- [34] H. R. Kang, *Computational Color Technology*. Bellingham, WA, USA: SPIE Press, 2006, pp. 151–182.
- [35] G. Wyszecki and W. S. Stiles, *Color Science*, 2nd ed. New York, NY, USA: Wiley, 1982.
- [36] K. Lee, C. Kim, and J.-I. Park, "Infrared-camera-based metamer marker for use in dark environments," in *Proc. IEEE Int. Conf. Consum. Electron. (ICCE)*, Jan. 2018, pp. 1–3.
- [37] S. I. Nin, J. M. Kasson, and W. Plouffe, "Printing CIELAB images on a CMYK printer using tri-linear interpolation," *Proc. SPIE*, vol. 1670, pp. 316–324, May 1992.
- [38] J. M. Kasson, S. I. Nin, W. Plouffe, and J. L. Hafner, "Performing color space conversions with three-dimensional linear interpolation," *J. Electron. Imag.*, vol. 4, no. 3, pp. 226–250, 1995.
- [39] E. Reinhard, M. Adhikhmin, B. Gooch, and P. Shirley, "Color transfer between images," *IEEE Comput. Graph. Appl.*, vol. 21, no. 5, pp. 34–41, Jul./Aug. 2001.
- [40] P. C. Hung, "Colorimetric calibration in electronic imaging devices using a look-up-table model and interpolation," *SPIE J. Electron. Imag.*, vol. 2, no. 1, pp. 53–61, Jan. 1993.
- [41] R. D. Hersch, "Spectral prediction model for color prints on paper with fluorescent additives," *Appl. Opt.*, vol. 47, no. 36, p. 6710, Dec. 2008.
- [42] R. D. Hersch, P. Donz, and S. Chosson, "Color images visible under UV light," *ACM Trans. Graph.*, vol. 22, no. 3, pp. 427–436, 2007.
- [43] M. Billingham, H. Kato, and I. Poupyrev, "The MagicBook: Moving seamlessly between reality and virtuality," *IEEE Comput. Graph. Appl.*, vol. 21, no. 3, pp. 6–8, May 2001.
- [44] R. M. Yilmaz, S. Kucuk, and Y. Goktas, "Are augmented reality picture books magic or real for preschool children aged five to six?" *Brit. J. Educ. Technol.*, vol. 48, no. 3, pp. 824–841, May 2017.



**KANGHOON LEE** received the B.S. degree in multimedia engineering from Hansung University, Seoul, South Korea, in 2008. He is currently pursuing the Ph.D. degree with Hanyang University. His major interests are image processing and computer vision. His main research topics include AR applications, human–computer interaction, colors, computer vision, and digital culture heritage.



**KYUDONG SIM** received the B.S. degree in electronics from Hanyang University, Seoul, South Korea, in 2015, where he is currently pursuing the Ph.D. degree. His major interests are image processing and computer vision. His main research topics include colors, multispectral imaging, computer vision, and AR applications.



**TAEYOUNG UHM** received the B.S. degree in electrical engineering from Kyonggi University, Suwon, South Korea, in 2004, and the M.S. and Ph.D. degrees in electronics and computer engineering from Hanyang University, Seoul, South Korea, in 2006 and 2014, respectively. From 2014 to 2017, he was a Researcher with the Korea Institute of Science and Technology, Seoul. In 2017, he joined the Smart Mobility Research Center, Korea Institute of Robotics & Technology Convergence, Pohang, South Korea, where he is currently a Senior Researcher. His current research interests include robotics, autonomous navigation, multimodal 3-D motion estimation, emotion recognition, and human–robot interaction.



Sang Hwa Lee received the *IEEE* Chester Sall 3rd place Award, in 2014.

**SANG HWA LEE** received the B.S. and M.S. degrees in electronics and the Ph.D. degree in electrical engineering from Seoul National University, Seoul, South Korea, in 1994, 1996, and 2000, respectively. He has been a Research Professor with Seoul National University, since 2005. His major interests are image processing and computer vision. His main research topics include stereo camera systems, MRF modeling, image restoration and enhancement, pattern recognition, consumer electronics, and VR/AR applications. He received the *IEEE* Chester



Jong-Il Park received the B.S., M.S., and Ph.D. degrees in electronics engineering from Seoul National University, South Korea, in 1987, 1989, and 1995, respectively. He enjoyed doing research at the NHK Science and Technology Research Laboratories, Tokyo, from 1992 to 1994. In 1995, he was with the Korean Broadcasting Institute. From 1996 to 1999, he was involved in various projects on AR/VR and 3D computer vision at the ATR Media Integration and Communication Research Laboratories, Kyoto, Japan. In 1999, he joined Hanyang University, Seoul, South Korea, where he is currently a Professor with the Department of Computer Science. During sabbatical leaves, he worked at the University of Florence, Italy, The University of Tokyo, Japan, Columbia University, USA, and LG Electronics, South Korea. He has published more than 200 refereed articles in the field of computer vision/graphics, virtual and augmented reality, computational imaging and display, and human-computer interaction.

• • •